National Défense
Defence nationale

UNCLASSIFIED

DRES

≡SUFFIELD MEMORANDUM≡

NO. 1348

AD-A231 386

FINITE DIFFERENCE FORM OF THE COMPRESSIBLE

BOUNDARY LAYER EQUATIONS IN GENERALIZED

CURVILINEAR COORDINATES

by

Denis Bergeron

DTIC
ELECTE
JAN 23 1991
S E D

December 1990

DEFENCE RESEARCH ESTABLISHMENT SUFFIELD, RALSTON, ALBERTA

Canada

Defence Research Establishment Suffield
Ralston, Alberta

Suffield Memorandum No. 1348

Finite Difference Form of the Compressible Boundary Layer Equations in Generalized Curvilinear Coordinates

by

Denis Bergeron

Accession For	
NTIS GRA&I	☒
DTIC TAB	☐
Unannounced	☐
Justification	

By

Distribution/

Availability Codes	
Avail and/or	
Dist	Special
A-1	

ABSTRACT

This paper presents the development of a finite difference form of the unsteady boundary layer equations for two-dimensional flow. The equations are written in body-conformal coordinates, non-dimensionalized, transformed to a generalized curvilinear coordinate system, and expanded to yield equations suitable for use in a tridiagonal solver. The boundary conditions are also presented.

This work, done in cooperation with the University of Toronto, seeks the development of a boundary layer code compatible with the NASA Ames ARC2D Navier-Stokes code. The two codes will be used in a study of the Fortified Navier-Stokes concept.

RÉSUMÉ

Cette communication porte sur le développement d'une forme aux différences finies des équations des couches limites instables dans les écoulements bidimensionnels. Les équations sont exprimées en coordonnées conformes au corps étudié, sans dimension, sont transformées en un système de coordonnées curvilinéaires généralisées et sont développées en équations applicables à un résolveur tridiagonal. Les conditions aux limites sont aussi présentées.

Ce travail, mené en collaboration avec l'Université de Toronto, vise à élaborer un programme de couche limite compatible avec le programme Navier-Stokes ARC2D mis au point par l'Ames pour la NASA. Les deux programmes serviront à étudier le concept fortifié de Navier-Stokes.

TABLE OF CONTENTS

LIST OF FIGURES

NOMENCLATURE

A,B,C,D	Coefficients of tridiagonal system of equations
a	Speed of sound
c_p	Coefficient of specific heat at constant pressure
H	Total enthalpy, $H = c_p + u^2/2$
l	Reference length
M	Mach number, $M = u/a$
p	Pressure
Pr	Prandtl number, $Pr = \mu c_p/\kappa$
R	Gas constant
Re	Ratio of freestream Reynolds and Mach numbers, $\text{Re} = \rho_\infty l a_\infty/\mu_\infty$
S_1	Constant used in Sutherland's approximation for viscosity
t	Time-like variable used to relax the equations
T	Absolute temperature
u,v	Body-conformal velocity components
U,V,W	Contraviariant velocity components
x,y	Body-conformal coordinates
X,Y	Cartesian coordinates

Greek Symbols

α	Convective coefficient, $\alpha = \rho U$
γ	Ratio of specific heat at constant pressure to specific heat at constant volume
κ	Coefficient of thermal conductivity
μ	Viscosity
ρ	Density
τ	Shear stress, $\tau = \mu(\partial u/\partial y)$
ξ,η	Curvilinear coordinates

Subscripts

$()_0$	Reference conditions in Sutherland's approximation
$()_\infty$	Freestream values
$()_j, ()_k$	Dummy spacial indices
$()_w$	Value at a solid boundary (wall)
$()_{wc}$	Value at the wake centerline

Superscripts

$(\tilde{\ })$	Non-dimensionalized value
$()^n$	Dummy time index

INTRODUCTION

Background

Throughout the Computational Fluid Dynamics community, two approaches to the numerical simulation of viscous flow have gained popularity: the Interactive Boundary Layer (IBL) approach and the Navier-Stokes approach.

IBL methods solve separate inviscid and viscid solutions, which influence each other throught an interaction algorithm. The interaction is allowed to continue until continuity of the velocity and temperature profiles is achieved at an interface boundary, usually the boundary layer edge. Numerical implementation of the method involves coding of separate solution algorithms for the inviscid and viscid regions, each based on specialized equations which approximate the Navier-Stokes equations under the conditions prevailing in that region. The viscous method also requires special adaptations for separated flow regions, where the boundary layer equations must be solved in inverse mode. This results in substantial human intervention to adapt a given code to a new class of problems.

Navier-Stokes methods solve the Navier-Stokes equations throughout the field. Their numerical implementation is simpler since a single set of equations applies to all regions of the flow field, but grid points must be concentrated in the viscous regions to resolve the boundary layer flow. Since the Navier-Stokes equations describe the physics for most aerodynamic problems, minimal human intervention is normally required to adapt a given code to a new class of problems.

It is recognized that IBL schemes require much less computer work per grid point and less computer storage than Navier-Stokes solvers to obtain a solution. However, they are more specialized and are restricted to computation of attached and mildly separated flows. When substantial flow separation exists, the less efficient, and more expensive Navier-Stokes methods must be used.

Hence, Navier-Stokes codes are quite general in their range of application but they are expensive to run. As a result, most Navier-Stokes codes require improvements to reduce the associated computational workload. On the other hand, IBL methods are efficient, but the equations used may not describe the physics of the flow adequately. These codes require improvements to produce more realistic simulations.

Fortified Navier-Stokes Approach

Over the past decade, NASA Ames researchers used a boundary layer solution as a forcing function to the Thin Layer Navier-Stokes (TLNS) equations to improve the convergence characteristics of their Navier-Stokes code. They called this approach "Fortified Navier-Stokes" (FNS).

Conceptually, a FNS code is a standard Navier-Stokes code which solves the TLNS equations throughout the computational domain. However, the TLNS equations have been modified to incorporate approximate solutions (e.g. for a boundary layer equations) in zones where they cleary apply. As a result, the FNS code can be used in a way similar to an IBL code. An inviscid solution is obtained by solving the TLNS equations on a coarse grid. Coarseness of the grid prevents accurate resolution of the viscous terms within the boundary layer region. To recover this information, the boundary layer equations are solved using a fine mesh overlay near the airfoil surface, and the solution is impressed on the inviscid solution through a forcing function term added to the standard TLNS equations. The advantage of a FNS code is that, should the boundary layer assumption break down, the forcing term can be set to zero and computations can continue using the conventional Navier-Stokes solution on a refined grid. Steger and Van Dalsem developed several FNS code versions in 1985[1], 1986[2] and 1988[3], which differ by the form of the boundary layer equations used.

Previous Generalized Boundary Layer Work

Several boundary layer methods (e.g. Cebeci[4]) employ coordinate transformation, or "stretching" of the governing equations prior to formulation of the finite difference equations. The purpose is to scale the growth of the viscous layer so that the new equations, expressed in terms of similarity variables, may be solved on an approximately rectangular grid. Van Dalsem and Steger[5] took a different approach. They developed a scheme to solve the two-dimensional, steady state boundary layer equations in body-conformal coordinates (x,y), which amounts to solving the equations in physical - instead of similarity - variables. An adaptive grid must then be used to concentrate a sufficient number of computational points within the boundary layer. Solution of the equations on a grid with uneven spacing results in complicated finite difference equations, but this is avoided by transforming the equations to a computational domain with uniform grid spacing so that standard, unweighted differences can be used.

The scheme of Van Dalsem and Steger is noteworthy for two reasons. First, it assumes the equations are only weakly coupled when the τ_w, is given. This allows them to solve each equation independently in a sequential scheme. They also chose their finite difference operators to allow use of efficient bidiagonal and tridiagonal solvers in the solution process.

Second, their scheme avoids use of complex space marching procedures within separated flow regions. Instead, the scheme marches in the general downstream direction while flow-dependent finite difference operators adapt locally to respect the parabolic nature of the boundary layer equations.

The earlier work of Steger and Van Dalsem[1][5] used a predictor-corrector finite difference approximation to the two-dimensional, steady state equations. They also used three types of operators depending on the local value of u/u_e. In 1986[2] and 1987[6], they expanded the equations to the three-dimensional unsteady form. They also simplified the formulation to a single-step process and only two operators dependent on the sign of the contravariant velocity U

or W. The time variable is not used in a true time fashion, since the method still assumes that the pressure distribution is fixed and given. Instead, the "time-like" variable is used to relax the equations. The magnitude of the "time step" affects the convergence rate.

In 1983, Steger and Van Dalsem[3] developed a completely different approach to solving the boundary layer equations. The boundary layer equations were recast in a form using the Cartesian velocity components instead of the usual boundary layer components. They can then be solved on a Cartesian grid, thus, increasing commonality with Navier-Stokes codes.

In the present work, the 1986 version of the generalized boundary layer equations is used. It was selected because it is simpler to implement than the 1988 formulation and will provide a framework from which to study numerical convergence issues. However, the equations are scaled differently than in references 3 and 6 to increase their compatibility with Pulliam's[7] Navier-Stokes code, ARC2D, with which the current generalized boundary layer code will be integrated. The equations are also expanded in sufficient detail for use directly in a computer program. Handling of the boundary conditions is also presented.

GOVERNING EQUATIONS

Equations in Body-Conformal Coordinates

We now set to write the two-dimensional form of the unsteady, compressible boundary layer equations in generalized curvilinear coordinates. We start from the dimensional Cartesian form of the equations as developed in standard fluid dynamics texts[8]

$$\rho \left[\frac{\partial u}{\partial t} + u \frac{\partial u}{\partial x} + v \frac{\partial u}{\partial y} \right] = -\frac{\partial p}{\partial x} + \frac{\partial}{\partial y} \left[\mu \frac{\partial u}{\partial y} \right] \qquad (1.a)$$

$$\rho c_p \left[\frac{\partial T}{\partial t} + \frac{\partial T}{\partial x} + v \frac{\partial T}{\partial y} \right] = \frac{\partial}{\partial y} \left[\kappa \frac{\partial T}{\partial y} \right] + \mu \left(\frac{\partial u}{\partial y} \right)^2 + \frac{\partial p}{\partial t} + u \frac{\partial p}{\partial x} \qquad (1.b)$$

$$\frac{\partial \rho}{\partial t} + \frac{\partial (\rho u)}{\partial x} + \frac{\partial (\rho v)}{\partial y} = 0 \qquad (1.c)$$

In addition, we require two constitutive equations: the perfect gas law, and a relation linking viscosity with temperature

$$p = \rho R T \qquad (1.d)$$

$$\mu = \mu(T) \qquad (1.e)$$

For air, the relation between viscosity and temperature can be expressed by an interpolation formula based on D.M. Sutherland's theory of viscosity[8, p.328] given as

$$\frac{\mu}{\mu_0} = \left[\frac{T}{T_0} \right]^{3/2} \left[\frac{T_0 + S_1}{T + S_1} \right]$$

where μ_0 denotes the viscosity at the reference temperature T_0. S_1 is a constant which, for air, is $S_1 = 110\,K$. This relation holds true for subsonic and supersonic flow, but not for hypersonic flow.

The independent variables x and y are the Cartesian coordinates; thus equation 1 applies to flow over a flat plate. However, by mapping the Cartesian grid to a body-conformal grid (see fig.1), the functional form of equation 1 remains valid as long as the surface has mild curvature (e.g. the rounded leading edge of an airfoil, but not around the trailing edge). In a body-conformal grid, the x coordinate is defined as the arc length along a solid surface (or along the dividing streamline of an airfoil wake), while the y coordinate is the distance normal to the body surface (or wake-dividing streamline) and is defined positive in the outward direction. The Cartesian to body-conformal mapping of the grid assumes the range of the y coordinates is much smaller than the range of the x coordinates. The difference in arc length between the lines defining the body surface ($y = 0$) and the line defining the outer edge of the Cartesian grid ($y = y_{max}$) is negligible.

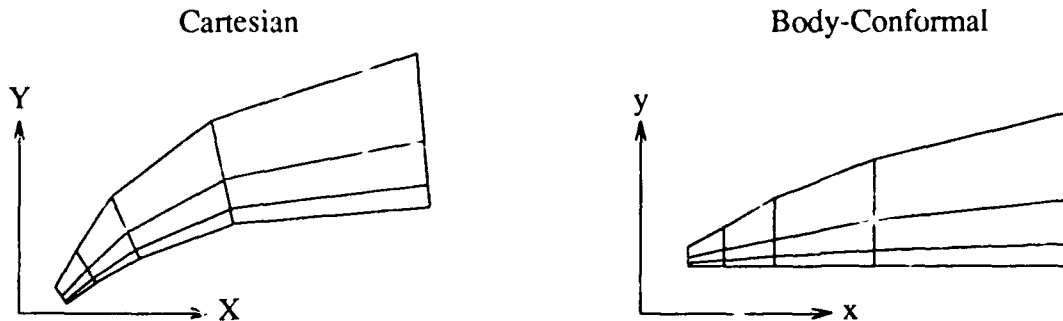Cartesian   Body-Conformal

Figure 1. Cartesian and Body-Conformal Coordinates

In their formulation, Steger and Van Dalsem[2][6] use the total enthalpy form of the energy equation (1.b). This form, derived in Appendix A, is

$$\rho \left[\frac{\partial H}{\partial t} + u \frac{\partial H}{\partial x} + v \frac{\partial H}{\partial y} \right] = \frac{\partial}{\partial y} \left[\frac{\mu}{Pr} \left[\frac{\partial H}{\partial y} + \frac{Pr - 1}{2} \frac{\partial (u)^2}{\partial y} \right] \right] \qquad (1.b)$$

Non-Dimensionalization of the Equations

To increase compatibility between the generalized boundary layer and Navier-Stokes codes, equation 1 is non-dimensionalized with the scaling used by Pulliam[7] in ARC2D. Density, viscosity and temperature are scaled by their freestream values as

$$\tilde{\rho} = \frac{\rho}{\rho_\infty} \quad ; \quad \tilde{\mu} = \frac{\mu}{\mu_\infty} \quad ; \quad \tilde{T} = \frac{T}{T_\infty}$$

Velocity, enthalpy and pressure are scaled by combinations of the freestream speed of sound and density as follows

$$\tilde{u} = \frac{u}{a_\infty} \quad ; \quad \tilde{v} = \frac{v}{a_\infty} \quad ; \quad \tilde{H} = \frac{H}{a_\infty^2} \quad ; \quad \tilde{p} = \frac{p}{\rho_\infty a_\infty^2}$$

Finally, the spacial coordinates are scaled by a reference length (usually the airfoil chord), l, and time is scaled by the same quantity divided by the freestream speed of sound, i.e.

$$\tilde{x} = \frac{x}{l} \quad ; \quad \tilde{y} = \frac{y}{l} \quad ; \quad \tilde{t} = \frac{t}{l/a_\infty}$$

Using the above scaling, equations (1.a-c) retain the same functional form except that the viscous terms of equations (1.a,b) are now divided by the ratio of Reynolds number to Mach number, defined as

$$\text{Re} = \frac{\rho_\infty a_\infty l}{\mu_\infty}$$

Note that the formal definition of the Reynolds number uses the freestream velocity u_∞ instead of the speed of sound a_∞. The standard Reynolds number is obtained by multiplying the above non-dimensional Re by the Mach number M_∞. In the remainder of this document, we drop the $\tilde{\ }$ for simplicity. The non-dimensional form of equations (1.a-c) is then

$$\rho \left[\frac{\partial u}{\partial t} + u \frac{\partial u}{\partial x} + v \frac{\partial u}{\partial y} \right] = -\frac{\partial p}{\partial x} + \frac{1}{\text{Re}} \frac{\partial}{\partial y} \left[\mu \frac{\partial u}{\partial y} \right] \qquad (2.a)$$

$$\rho \left[\frac{\partial H}{\partial t} + u \frac{\partial H}{\partial x} + v \frac{\partial H}{\partial y} \right] = \frac{1}{\text{Re}} \frac{\partial}{\partial y} \left[\frac{\mu}{Pr} \left[\frac{\partial H}{\partial y} + \frac{Pr-1}{2} \frac{\partial (u)^2}{\partial y} \right] \right] \qquad (2.b)$$

$$\frac{\partial \rho}{\partial t} + \frac{\partial (\rho u)}{\partial x} + \frac{\partial (\rho v)}{\partial y} = 0 \qquad (2.c)$$

The equation of state for a perfect gas (1.d) becomes

$$p = \frac{\rho T}{\gamma} \qquad (2.d)$$

where $T = (\gamma - 1)\left[H - \frac{(u^2 + v^2)}{2} \right]$ and γ is the ratio of specific heat ($\gamma = 1.4$ for air).

Because of its empirical nature, equation (1.e) cannot be expressed in terms of scaled variables only. However, if the freestream temperature is given, the following form is obtained

$$\mu = T^{3/2}\left[\frac{1 + S_1/T_\infty}{T + S_1/T_\infty} \right] \qquad (2.e)$$

Generalized Curvilinear Coordinates

A general curvilinear transformation is used to map the body-conformal coordinates (x,y) to computational coordinates (ξ,η), such that spacing in the computational domain is uniform and of unit length (see fig.2). Equations (2.a-c) are then transformed to general curvilinear coordinates

$$\xi = \xi(x)$$

$$\eta = \eta(x,y)$$

and solved on the computational domain using standard unweighted finite differences. The advantage of this transformation is that a single computational code can be used to solve the flow about a wide variety of physical geometries.

There normally exists a one-to-one correspondence between the body conformal and computational spaces. A notable exception is the wake cut when a C-grid geometry is applied to airfoils (see fig.3). Since the body-conformal space is obtained by "cutting" physical space along the wake and "unwrapping" it to align the wake centerline and body surface along the body-conformal x axis, physical points along the wake, including the airfoil trailing edge, correspond to two boundary points in the computational domain. It is important to choose the wake points carefully. They should correspond closely to the physical wake centerline. Application of the boundary conditions for the current boundary layer algorithm is then greatly reduced, as will be discussed later.

Body-Conformal · Computational
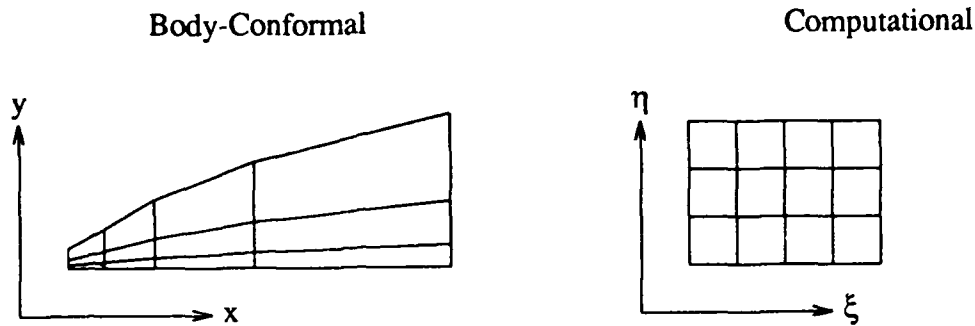
Figure 2. Body-Conformal and Computational Grids

Cartesian C-Grid · Computational Grid
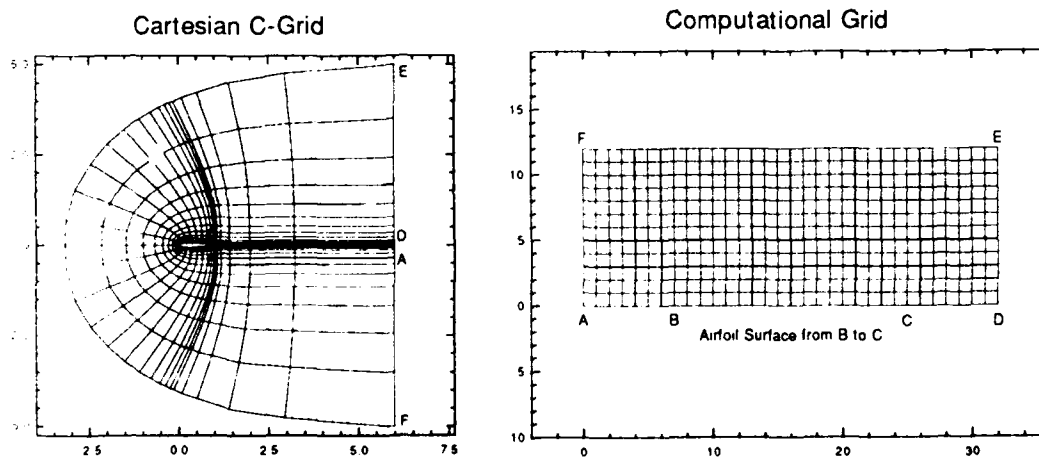
Figure 3. Mapping of C-Grid to Computational Domain

The chain rule is used to express the body-conformal derivatives (∂_x and ∂_y) of equations (2.a-c) in terms of the curvilinear derivatives

$$\partial_x = \xi_x \partial_\xi + \eta_x \partial_\eta$$

$$\partial_y = \eta_y \partial_\eta$$

Transformation of equations (2.a-c) using these derivatives yields

$$\rho\left[u_t + Uu_\xi + Vu_\eta\right] = -\xi_x p_\xi + \frac{1}{Re}\eta_y\left[\mu\eta_y u_\eta\right]_\eta \qquad (3.a)$$

$$\rho\left[H_t + UH_\xi + VH_\eta\right] = \frac{1}{Re}\eta_y\left[\frac{\mu}{Pr}\left[\eta_y H_\eta + \frac{Pr-1}{2}\eta_y(u^2)_\eta\right]\right]_\eta \qquad (3.b)$$

$$\rho_t + \xi_x(\rho u)_\xi + \eta_x(\rho u)_\eta + \eta_y(\rho v)_\eta = 0 \qquad (3.c)$$

where U and V are the contravariant velocities defined as

$$U = \xi_x u$$

$$V = \xi_y u + \eta_y v$$

The equation of state (2.d) and the Sutherland formula (2.e) are not affected by the transformation.

Equations (3.a-c) are similar to those of references 3 and 6 with the exception that scaling of the pressure and viscous terms is changed. In the next section, we apply the 1986 version of the Steger and Van Dalsem finite difference scheme to the current equations and obtain the finite difference equations required for coding.

NUMERICAL FORMULATION

Steger and Van Dalsem[2][6] developed a time-like algorithm to solve the boundary layer equations. Their method assumes that pressure is known. This allows decoupling of the equations which are then solved sequentially at each time step or cycle. Furthermore, the algorithm was selected so that scalar tridiagonal systems of equations are solved for each equation. Time derivatives are first-order accurate while spacial derivatives in the momentum and energy equations are approximated by centered differences in the η direction and by flow-dependent upwind differences in the ξ direction. At any ξ station, the upwind direction is determined from the sign of the coefficient ρU. A backward difference is used if ρU is positive and a forward difference is used if ρU is negative.

The term $(\rho v)_\eta$ of the continuity equation is integrated in the η direction using the trapezoidal rule. The ξ and η derivatives for the (ρu) terms are approximated by second-order accurate centered differences.

Details of the algorithm are now presented for each equation, separately, using conventional operators defined in terms of the shift operator E, e.g. $E_\xi^{\pm 1} u_j = u_{j \pm 1}$

$$\nabla_\xi = \frac{1 - E_\xi^{-1}}{\Delta \xi}$$

$$\Delta_\xi = \frac{E_\xi^{+1} - 1}{\Delta \xi}$$

$$\delta_\xi = \frac{E_\xi^{+1} - E_\xi^{-1}}{2 \Delta \xi}$$

$$\bar{\delta}_\xi = \frac{E_\xi^{+\frac{1}{2}} - E_\xi^{-\frac{1}{2}}}{\Delta \xi}$$

and the second-order accurate upwind operator

$$\widehat{\alpha \hat{\delta}_\xi} = \left(\frac{\alpha + |\alpha|}{2} \right) \nabla_\xi \left(\frac{3 - E_\xi^{-1}}{2} \right) + \left(\frac{\alpha - |\alpha|}{2} \right) \Delta_\xi \left(\frac{3 - E_\xi^{+1}}{2} \right)$$

where α is the convective coefficient ρU.

Finally, we use the convention that space or time indices are written only if changed, i.e. $u = u_{j,k}^n$, $u^{n+1} = u_{j,k}^{n+1}$, etc.

Momentum Equation

General Form

Within the main field (i.e. away from boundaries), the finite difference form of equation (3.b) is given by

$$\rho\left[\nabla_t u^{n+1} + \hat{U}\hat{\delta}_\xi u^{n+1} + V\delta_\eta u^{n+1}\right] = -\xi_x \delta_\xi p + \frac{1}{Re}\eta_y \bar{\delta}_\eta\left[\mu\eta_y \bar{\delta}_\eta u^{n+1}\right]$$

To be solved numerically, the above equation must be expanded in terms of the numerical values, which, after rearranging, leads to the following form

$$\left[-\frac{\rho V}{2} - \frac{\eta_y}{Re}\left[\frac{(\mu\eta_y) + (\mu\eta_y)_{k-1}}{2}\right]\right] u_{k-1}^{n+1}$$

$$+\left[\frac{\rho}{\Delta t} + \rho\left[\frac{U+|U|}{2}\right]\frac{3}{2} - \left[\frac{U-|U|}{2}\right]\frac{3}{2} + \frac{\eta_y}{Re}\left[\frac{(\mu\eta_y)_{k-1} + 2(\mu\eta_y) + (\mu\eta_y)_{k+1}}{2}\right]\right] u^{n+1}$$

$$+\left[\frac{\rho V}{2} - \frac{\eta_y}{Re}\left[\frac{(\mu\eta_y) + (\mu\eta_y)_{k+1}}{2}\right]\right] u_{k+1}^{n+1} \tag{4.a}$$

$$= -\xi_x\left[\frac{p_{j+1} - p_{j-1}}{2}\right] - \rho\left[\frac{U+|U|}{2}\right]\left[\frac{-4u_{j-1} + u_{j-2}}{2}\right] - \rho\left[\frac{U-|U|}{2}\right]\left[\frac{4u_{j+1} - u_{j+2}}{2}\right]$$

Equation (4.a) is solved implicitly at each ξ station. Thus, a tridiagonal set of equations is obtained by solving this equation for the points $\eta = 2$ to $\eta = \eta_{max-1}$.

Use of equation (4.a) near the ξ boundaries is unacceptable numerically. For example, at the $\xi = 1$ boundary, the variables u_{j-1}, u_{j-2} and p_{j-1} reference values outside of the numerical arrays U() and P(). This introduces errors and usually leads to numerical instability. At this point, it is useful to consider the treatment of equation (4.a) near the boundaries of the computational domain.

ξ Boundary Condition

The choice of boundary conditions depends on the flow characteristics of the physical domain and the choice of grid topology. The C-grid used in the present work extends far enough into the wake to ensure that outflow conditions exist at the ξ boundaries. This means that forward

differencing of the ρU term is used at $\xi = 1$ and backward differencing is used at $\xi = \xi_{max}$. Nevertheless, the numerics require that the second-order accurate upwind operator be modified at the $\xi = 1,2,\xi_{max-1}$ and ξ_{max} points. The modified operators are

$$\xi = 1: \quad \hat{\alpha}\hat{\delta}_\xi = \left[\frac{\alpha - |\alpha|}{2}\right] \Delta_\xi \left[\frac{3 - E_\xi^{+1}}{2}\right]$$

$$\xi = 2: \quad \hat{\alpha}\hat{\delta}_\xi = \left[\frac{\alpha + |\alpha|}{2}\right] \nabla_\xi + \left[\frac{\alpha - |\alpha|}{2}\right] \Delta_\xi \left[\frac{3 - E_\xi^{+1}}{2}\right]$$

$$\xi = \xi_{max-1}: \quad \hat{\alpha}\hat{\delta}_\xi = \left[\frac{\alpha + |\alpha|}{2}\right] \nabla_\xi \left[\frac{3 - E_\xi^{-1}}{2}\right] + \left[\frac{\alpha - |\alpha|}{2}\right] \Delta_\xi$$

$$\xi = \xi_{max}: \quad \hat{\alpha}\hat{\delta}_\xi = \left[\frac{\alpha + |\alpha|}{2}\right] \nabla_\xi \left[\frac{3 - E_\xi^{-1}}{2}\right]$$

The above modifications to the streamwise convective derivatives ensure that only points within the computational domain are used. Hence, only first-order differences are used to approximate inflow derivatives at the $\xi = 2$ and $\xi = \xi_{max-1}$ stations. Dropping the backward difference at the $\xi = 1$ station and the forward difference at the $\xi = \xi_{max}$ may not be physically acceptable, but it is necessary numerically. The onus is on the user to make sure that outflow conditions prevail at these stations.

To test coding of the algorithm, other grid types may be used and inflow conditions may exist at one of the ξ boundaries. Such is the case for the computation of the flow over a flat plate. In this case, upstream data must be supplied (e.g. for stations $\xi = 1,2$ if ρU is positive).

Treatment of the pressure terms at the ξ boundaries simply consists of replacing the centered difference by a forward difference at $\xi = 1$ and by a backward difference at $\xi = \xi_{max}$. Since the pressure terms are known *a priori*, they do not affect the tridiagonal nature of the algorithm and second-order accurate differences are used as follows

$$p_\xi|_1 = \Delta_\xi \left[\frac{3 - E_\xi^{+1}}{2}\right] p$$

$$p_\xi|_{\xi_{max}} = \nabla_\xi \left[\frac{3 - E_\xi^{-1}}{2}\right] p$$

η Boundary Condition

Two distinct boundary conditions are applied along the $\eta = 1$ line. The no-slip condition, $(u_1 = 0)$, is used for points on the surface of the airfoil. Thus, at the $\eta = 2$ point, equation (4.a) is expressed as

$$A_2 u_1 + B_2 u_2 + C_2 u_3 = D_2$$

where A_2, B_2, C_2 are the coefficients of u_{k-1}^{n+1}, u^{n+1} and u_{k+1}^{n+1} respectively in equation (4.a). D_2 represents the right hand side of the equation. With u_1 set equal to zero, the first term simply disappears from the equation.

In the wake, the boundary condition $u_y |_1 = 0$ is used. This derivative may be expressed as a second-order accurate forward difference in η, i.e.

$$u_y |_1 = \Delta_\eta \left[\frac{3 - E_\eta^{+1}}{2} \right] u^{n+1} = 0$$

A value for u_1 in terms of u_2 and u_3 is obtained from the above equation. It is substituted in the coefficient form of equation (4.a) at $\eta = 2$, which yields

$$\left[\frac{4A_2}{3} + B_2 \right] u_2 + \left[C_2 - \frac{A_2}{3} \right] u_3 = D_2 \qquad (4a,1)$$

Locally, the tridiagonal form of the system of equations is preserved.

At the upper η boundary ($\eta = \eta_{max}$), the standard boundary layer edge condition $u_y |_e$ is used. The same logic used to derive the wake centerline boundary condition yields the following coefficient form of equation (4.a)

$$\left[A_{K_{max}-1} - \frac{C_{K_{max}-1}}{3} \right] u_{K_{max}-1} + \left[B_{K_{max}-1} + \frac{4C_{K_{max}-1}}{3} \right] u_{K_{max}-1} = D_{K_{max}-1} \quad (4.a,2)$$

Inverse Formulation

Near and in regions of reverse flow, the pressure gradient term of equation (4.a) must be replaced by an inverse forcing function. Steger and Van Dalsem use the wall shear stress, τ_w, on the airfoil surface and the wake centerline velocity, u_{wc} in the wake. These expressions are

obtained by applying the momentum equation at the airfoil surface, which yields the following relation

$$\xi_x p_\xi = \frac{\eta_y}{Re}\left[\mu\eta_y u_\eta\right]_\eta \bigg|_w \tag{5.a}$$

$$= \frac{2}{Re}\left[\frac{\dfrac{\mu_1+\mu_2}{2}\dfrac{u_2-u_1}{y_2-y_1}-\tau_w}{y_2-y_1}\right]$$

Note that $u_1 = 0$ and that τ_w is scaled by $\dfrac{l}{(\mu_\infty a_\infty)}$. At the wake centerline, the equivalent relation is

$$\xi_x p_\xi = \left[\frac{\eta_y}{Re}\left[\mu\eta_y u_\eta\right]_\eta - \rho U u_\xi\right]\bigg|_{wc} \tag{5.b}$$

$$= \frac{2}{Re}\left[\frac{\dfrac{\mu_1+\mu_2}{2}\dfrac{u_2-u_1}{y_2-y_1}-\tau_w}{y_2-y_1}\right] - \left[\rho\hat{U}\hat{\delta}_\xi u\right]\bigg|_{wc}$$

where $u_1 = u_{wc}$, $\tau_w = 0$, and $U|_{wc} = \xi_x u_{wc}$

The presence of a u_2 term in the inverse forcing functions results in an augmented tridiagonal system of equations. Steger and Van Dalsem[4] developed an efficient lower-upper decomposition scheme to solve this particular system of equations.

Energy Equation

General Form
The finite difference scheme used for the momentum equation is now applied to equation (3.b), the energy equation. Using the finite difference operators defined previously, we obtain

$$\rho\left[\nabla_t H^{n+1} + \hat{U}\hat{\delta}_\xi H^{n+1} + V\delta_\eta H^{n+1}\right] = \frac{\eta_y}{Re}\bar{\delta}_\eta\left[\frac{\mu}{Pr}\left[\eta_y\bar{\delta}_\eta H^{n+1} + \frac{Pr-1}{2}\eta_y\bar{\delta}_\eta(u^{n+1})^2\right]\right]$$

Expanding this equation in terms of the field values, and rearranging to the tridiagonal (in η) coefficient form , we obtain

$$\left[-\frac{\rho V}{2} - \frac{\eta_y}{2\,\mathrm{Re}}\left[\left[\frac{\mu\eta_y}{Pr}\right] + \left[\frac{\mu\eta_y}{Pr}\right]_{k-1}\right]\right] H_{k-1}^{n+1}$$

$$+ \left[\frac{\rho}{\Delta t} + \rho\left[\frac{U+|U|}{2}\right]\frac{3}{2} - \rho\left[\frac{U-|U|}{2}\right]\frac{3}{2} + \frac{\eta_y}{2\,\mathrm{Re}}\left[\left[\frac{\mu\eta_y}{Pr}\right]_{k-1} + 2\left[\frac{\mu\eta_y}{Pr}\right] + \left[\frac{\mu\eta_y}{Pr}\right]_{k+1}\right]\right] H^{n+1}$$

$$+ \left[\frac{\rho V}{2} - \frac{\eta_y}{2\,\mathrm{Re}}\left[\left[\frac{\mu\eta_y}{Pr}\right] + \left[\frac{\mu\eta_y}{Pr}\right]_{k+1}\right]\right] H_{k+1}^{n+1} \qquad (4.b)$$

$$= \frac{\eta_y}{2\,\mathrm{Re}}\left[\frac{Pr-1}{2}\right]\left[\left[\left[\frac{\mu\eta_y}{Pr}\right]_{k+1} + \left[\frac{\mu\eta_y}{Pr}\right]\right]\left[u_{k+1}^2 - u^2\right] - \left[\left[\frac{\mu\eta_y}{Pr}\right]_{k-1} + \left[\frac{\mu\eta_y}{Pr}\right]\right]\left[u^2 - u_{k-1}^2\right]\right]$$

The solution scheme for equation (4.b) is the same as that for equation (4.a). An implicit system of equations in η is solved at each ξ station. Also, the restriction on the numerical values of $H_{j\pm1}$ and $H_{j\pm2}$ near the ξ boundaries are the same as for the momentum equation.

Boundary Conditions
The explanation given for the ξ boundary conditions of the momentum equation also holds true for the energy equation. Two boundary conditions may be applied along the $\eta = 1$ boundary. The wall and wake centerline may be specified (T_w and T_{wc} given) or adiabatic conditions may be used ($T_y|_w$ and $T_y|_{wc}$ set to zero). In the present work, the adiabatic condition is used throughout the domain which leads to the condition

$$H_y|_w = H_y|_{wc} = 0$$

or,

$$\left[\frac{4}{3}A_2 + B_2\right] H_2 + \left[C_2 - \frac{A_2}{3}\right] H_3 = D_2 \qquad (4b,1)$$

Continuity Equation

The continuity equation (3.c) is rearranged to isolate the (ρv) term on the left-hand side of the equal sign as follows

$$(\rho v)_\eta = -\frac{\left[\xi_x(\rho u)_\xi + \eta_x(\rho u)_\eta + \rho_t\right]}{\eta_y}$$

The right-hand side is then a function of the variables ρ and u alone, which are presumed known. The trapezoidal rule is used to integrate (ρv) in the η direction starting from the $\eta = 1$ line where v_w is known to be zero on the airfoil, due to the no-slip condition, and v_{wc} is assumed to be zero due to the symmetry condition in the wake, condition which should be satisfied if the wake cut location is selected carefully. This leads to the folowing finite difference equation

$$\nabla_\eta(\rho v)^{n+1} = -\left[\frac{1+E_\eta^{-1}}{2}\right]\left[\frac{\xi_x\delta_\xi(\rho u) + \eta_x\delta_\eta(\rho u) + \nabla_t\rho}{\eta_y}\right]^{n+1}$$

Expanding the above equation in terms of field variables, we obtain an explicit equation for (ρv)

$$(\rho v) - (\rho v)_{k-1} = \qquad\qquad\qquad\qquad\qquad\qquad\qquad\qquad\qquad (4.c)$$

$$-\left[\frac{\xi_x}{2}\left[(\rho u)_{j+1}^{n+1} - (\rho u)_{j-1}^{n+1}\right] + \frac{\eta_x}{2}\left[(\rho u)_{k+1}^{n+1} - (\rho u)_{k-1}^{n+1}\right] + \frac{\rho^{n+1} - \rho}{\Delta t}\right] / \eta_y$$

$$-\left[\frac{\xi_{x\,k-1}}{2}\left[(\rho u)_{j+1,k-1}^{n+1} - (\rho u)_{j-1,k-1}^{n+1}\right] + \frac{\eta_{x\,k-1}}{2}\left[(\rho u)^{n+1} - (\rho u)_{k-2}^{n+1}\right] + \frac{\rho_{k-1}^{n+1} - \rho_{k-1}}{\Delta t}\right] / \eta_{y\,k-1}$$

Centered differences in ξ and η are used throughout the field to approximate the (ρu) derivatives. At the boundaries, centered derivatives are replaced by second-order accurate forward or backward differences to respect the constraints imposed by the numerical method, i.e. that only points within the computational domain be used. This includes the following cases:

[1]   At $\xi = 1$: Replace $\delta_\xi(\rho u)$ by $\Delta_\xi\left[\dfrac{3 - E_\xi^{+1}}{2}\right](\rho u)$

[2] At $\xi = \xi_{max}$: Replace $\delta_\xi(\rho u)$ by $\nabla_\xi \left[\dfrac{3 - E_\xi^{-1}}{2} \right] (\rho u)$

[3] At $\eta = 2$: Replace $\delta_\eta(\rho u)_{k-1}$ by $\Delta_\eta \left[\dfrac{3 - E_\eta^{+1}}{2} \right] (\rho u)_{k-1}$

[4] At $\eta = \eta_{max}$: Replace $\delta_\eta(\rho u)$ by $\nabla_\eta \left[\dfrac{3 - E_\eta^{-1}}{2} \right] (\rho u)$

Application of equation (4.c) to points from $\eta = 2$ to $\eta = \eta_{max}$ yields a bidiagonal system of equations which is solved using the standard tridiagonal solver. The normal velocity distribution is finally obtained by dividing the result by the density.

Iterative Scheme

The iterative scheme used in the current implementation is identical to that used by Steger and Van Dalsem in their 1986-1987 version. It is repeated here for completeness.

[1] Solve the momentum equation (4.a), throughout the computational domain, to yield the u field at time n+1.

[2] Using the updated values of u (which also affect U and V), solve the energy equation (4.b) to obtain the H field at time n+1.

[3] Use the u^{n+1} and H^{n+1} values with the equation of state (2.d) to obtain ρ^{n+1}.

[4] Integrate the continuity equation (4.c) to get v^{n+1} which is also used to update the contravariant velocity V.

[5] Update the viscosity field μ using Sutherland's formula (2.e). For turbulent flow, the Baldwin-Lomax model[9] is also used to update the values of the apparent viscosity μ_t due to the Reynolds stresses.

References 3 and 6 are not specific about the method used to sweep the computational field. For example, it is not clear whether the flow field is swept in the general downstream direction from the forward stagnation point or if the sweeps are done from one end of the computational field to the other irrespective of the general flow direction. The equations developed in this paper will be used to investigate this.

FUTURE WORK

The finite difference equations approximating the compressible boundary layer equations in two dimensions have been developed in sufficient detail for use directly in a computer code. Development of a research code to study the convergence characteristics of these equations is underway. The iterative scheme outlined in section 3.4 will be used with various techniques to sweep the computational field.

The effect of the time-like variable used to relax the equations, as well as the treatment of the convective terms (ρU terms) in the momentum and energy equations, are not well understood. The new code will be used to study the effect of these terms on the overall convergence characteristics of the algorithm.

APPENDIX A

Enthalpy Form of the Energy Equation

A rigorous development of the enthalpy form of the energy equation is done from the full Navier-Stokes equations. However, in the context of the boundary layer approximation to the enthalpy equation, the same result is achieved by using equations (1.a,b), which are already subject to the boundary layer assumption.

Our development starts with the addition of equation (1.b) and equation (1.a), the latter being multiplied by the velocity u as follows

$$\rho c_p \left[\frac{\partial T}{\partial t} + u \frac{\partial T}{\partial x} + v \frac{\partial T}{\partial y} \right] + \rho u \left[\frac{\partial u}{\partial t} + u \frac{\partial u}{\partial x} + v \frac{\partial u}{\partial y} \right] =$$

$$\frac{\partial}{\partial y} \left[\kappa \frac{\partial T}{\partial y} \right] + \mu \left[\frac{\partial u}{\partial y} \right]^2 + \frac{\partial p}{\partial t} + u \frac{\partial p}{\partial x} - u \frac{\partial p}{\partial x} + u \frac{\partial}{\partial y} \left[\mu \frac{\partial u}{\partial y} \right]$$

We first consider the left-hand side of the above equation. Terms like $u \frac{\partial u}{\partial t}$, $u \frac{\partial u}{\partial x}$ and $u \frac{\partial u}{\partial y}$ may be expressed as $\frac{\partial (u^2/2)}{\partial t}$, $u \frac{\partial (u^2/2)}{\partial x}$ and $u \frac{\partial (u^2/2)}{\partial y}$ respectively. Using the perfect gas relation $h = c_p T$, the constant c_p may be brought into the T derivatives and replaced by h. Total enthalpy is defined as $H = h + (u^2 + v^2)/2$, but the v^2 term is neglected under the boundary layer assumption. Hence the left-hand side of the equation becomes

$$\rho \left[\frac{\partial H}{\partial t} + u \frac{\partial H}{\partial x} + v \frac{\partial H}{\partial y} \right]$$

The right-hand side of the equation is now considered. The $u \frac{\partial p}{\partial x}$ terms cancel out. The κ variable is replaced by its Prandtl number definition $\kappa = \mu c_p / Pr$. We also make use of the relation

$$u \frac{\partial}{\partial y}\left[\mu \frac{\partial u}{\partial y}\right] = \frac{\partial}{\partial y}\left[\mu \frac{\partial(u^2/2)}{\partial y}\right] - \mu\left[\frac{\partial u}{\partial y}\right]^2$$

The $\mu\left[\dfrac{\partial u}{\partial y}\right]^2$ terms cancel out. Combining the terms within the y derivatives, the right-hand side of the equation becomes

$$\frac{\partial}{\partial y}\left[\frac{\mu c_p}{Pr} \frac{\partial T}{\partial y} + \mu \frac{\partial(u^2/2)}{\partial y}\right] + \frac{\partial p}{\partial t}$$

The constant c_p is brought within the T derivative and replaced by the enthalpy. We also add and subtract the term $\dfrac{\mu}{Pr} \dfrac{\partial(u^2/2)}{\partial y}$ within the y derivative. Rearranging, our equation (L.H.S. = R.H.S.) becomes

$$\rho\left[\frac{\partial H}{\partial t} + u \frac{\partial H}{\partial x} + v \frac{\partial H}{\partial y}\right] = \frac{\partial}{\partial y}\left[\frac{\mu}{Pr}\left[\frac{\partial H}{\partial y} + \frac{Pr - 1}{2} \frac{\partial(u^2)}{\partial y}\right]\right] + \frac{\partial p}{\partial t}$$

Finally, in the current numerical scheme, the pressure field is used as the forcing function to the momentum equation. It is assumed known and constant, hence the $\dfrac{\partial p}{\partial t}$ term is dropped.

REFERENCES

1. Steger, J.L. and Van Dalsem, W.R., "Developments in the Simulation of Separated Flows using Finite Difference Methods", Proceedings of the 3rd Symposium on Numerical and Physical Aspects of Aerodynamic Flows, California State University, Long Beach, California, 1985.

2. Van Dalsem, W.R. and Steger, J.L., "Using the Boundary Layer Equations in Three-Dimensional Viscous Flow Simulation", Proceedings of the 58th Meeting of the AGARD Fluid Dynamics Panel Symposium on Applications of Computational Fluid Dynamics in Aeronautics, Aix-en- Provence, France, 1986.

3. Steger, J.L. and Van Dalsem, W.R., "Navier-Stokes and Viscous-Inviscid Interaction", NASA CP 3020, Vol. I, Part 2, Symposium held at NASA Langley Research Center, Hampton, Virginia, April 19-21, 1988.

4. Cebeci, T. and Smith, A.M.O., "Analysis of Turbulent Boundary Layers", Academic Press, 1974.

5. Van Dalsem, W.R. and Steger, J.L., "Simulation of Separated Transonic Airfoil Flow by Finite-Difference Viscous-Inviscid Interaction", Ph.D. Thesis, Stanford Univ., 1984.

6. Van Dalsem, W.R. and Steger, J.L., "Efficient Simulation of Separated Three-Dimensional Viscous Flows Using the Boundary Layer Equations", AIAA J.Vol. 25, no. 3, pp. 395-400, 1987.

7. Pulliam, T.H., "Efficient Solution Methods for the Navier-Stokes Equations", Von Karman Institute for Fluid Dynamics Lecture Series: Numerical Techniques for Viscous Flow Computations, Brussels, Belgium, 1986.

8. Schlichting, H., "Boundary Layer Theory", 6th Ed., McGraw-Hill, 1968.

9. Baldwin, B.S. and Lomax, H., "Thin Layer Approximation and Algebric Model for Separated Turbulent Flows", AIAA 78-257, Paper presented at the 16th Aerospace Sciences Meeting, Huntsville, Alabama, 1978.

DOCUMENT CONTROL DATA

(Security classification of title, body of abstract and indexing annotation must be entered when the overall document is classified)

1. ORIGINATOR (the name and address of the organization preparing the document. Organizations for whom the document was prepared, e.g. Establishment sponsoring a contractor's report, or tasking agency, are entered in section 8.)	2. SECURITY CLASSIFICATION (overall security classification of the document. including special warning terms if applicable)
Defence Research Establishment Suffield Box 4000, Medicine Hat, Alberta T1A 8K6	Unclassified

3. TITLE (the complete document title as indicated on the title page. Its classification should be indicated by the appropriate abbreviation (S,C,R or U) in parentheses after the title.)

Finite Difference Form of the Compressible Boundary Layer
Equations in Generalized Curvilinear Coordinates (U)

4. AUTHORS (Last name, first name, middle initial. If military, show rank, e.g. Doe, Maj. John E.)

Bergeron, Denis

5. DATE OF PUBLICATION (month and year of publication of document) December 1990	6a. NO. OF PAGES (total containing information. Include Annexes, Appendices, etc.) 24	6b. NO. OF REFS (total cited in document) 9

6. DESCRIPTIVE NOTES (the category of the document, e.g. technical report, technical note or memorandum. If appropriate, enter the type of report, e.g. interim, progress, summary, annual or final. Give the inclusive dates when a specific reporting period is covered.)

Sufffield Memorandum No. 1348

8. SPONSORING ACTIVITY (the name of the department project office or laboratory sponsoring the research and development. Include the address.)

- - - - - - - - -

9a. PROJECT OR GRANT NO. (if appropriate, the applicable research and development project or grant number under which the document was written. Please specify whether project or grant) - - - - - - - - -	9b. CONTRACT NO. (if appropriate, the applicable number under which the document was written) - - - - - -
10a. ORIGINATOR'S DOCUMENT NUMBER (the official document number by which the document is identified by the originating activity. This number must be unique to this document.) SM 1348	**10b. OTHER DOCUMENT NOS.** (Any other numbers which may be assigned this document either by the originator or by the sponsor) - - - - - -

11 DOCUMENT AVAILABILITY (any limitations on further dissemination of the document, other than those imposed by security classification)

(X) Unlimited distribution
( ) Distribution limited to defence departments and defence contractors; further distribution only as approved
( ) Distribution limited to defence departments and Canadian defence contractors; further distribution only as approved
( ) Distribution limited to government departments and agencies; further distribution only as approved
( ) Distribution limited to defence departments; further distribution only as approved
( ) Other (please specify):

12. DOCUMENT ANNOUNCEMENT (any limitation to the bibliographic announcement of this document. This will normally correspond to the Document Availabilty (11). However, where further distribution (beyond the audience specified in 11) is possible, a wider announcement audience may be selected.)

Nil

13. **ABSTRACT** (a brief and factual summary of the document. It may also appear elsewhere in the body of the document itself. It is highly desirable that the abstract of classified documents be unclassified. Each paragraph of the abstract shall begin with an indication of the security classification of the information in the paragraph (unless the document itself is unclassified) represented as (S), (C), (R), or (U). It is not necessary to include here abstracts in both offical languages unless the text is bilingual).

This paper presents the development of a finite difference form of the unsteady boundary layer equations for two-dimensional flow. The equations are written in body conformal coordinates, non-dimensionalized, transformed to a generalized curvilinear coordinate system, and expanded to yield equations suitable for use in a tridiagonal solver. The boundary conditions are also presented.

This work, done in cooperation with the university of Toronto, seeks the development of a boundary layer code compatible with the NASA Ames ARC2D Navier-Stokes code. The two codes will be used in a study of the Fortified Navier-Stokes concept.

14. KEYWORDS, DESCRIPTORS or IDENTIFIERS (technically meaningful terms or short phrases that characterize a document and could be helpful in cataloguing the document. They should be selected so that no security classification is required. Identifiers, such as equipment model designation, trade name, military project code name, geographic location may also be included. If possible keywords should be selected from a published thesaurus. e.g. Thesaurus of Engineering and Scientific Terms (TEST) and that thesaurus-identified. If it is not possible to select indexing terms which are Unclassified, the classification of each should be indicated as with the title.)

BOUNDARY LAYER EQUATIONS

GENERALIZED CURVILINEAR COORDINATES

FINITE DIFFERENCE FORM